



UNIVERSITÀ DI PARMA

ARCHIVIO DELLA RICERCA

University of Parma Research Repository

Modeling of an Excavator System - Semi empirical hydraulic pump model

This is the peer reviewed version of the following article:

Original

Modeling of an Excavator System - Semi empirical hydraulic pump model / Casoli, Paolo; Anthony, Alvin; M., Rigosi. - In: SAE INTERNATIONAL JOURNAL OF COMMERCIAL VEHICLES. - ISSN 1946-391X. - 4:(2011), pp. 242-255. [10.4271/2011-01-2278]

Availability:

This version is available at: 11381/2378117 since: 2015-12-14T13:57:34Z

Publisher:

Published

DOI:10.4271/2011-01-2278

Terms of use:

Anyone can freely access the full text of works made available as "Open Access". Works made available

Publisher copyright

note finali coverpage

(Article begins on next page)

23 April 2024

Modeling of an Excavator System - Semi Empirical Hydraulic Pump Model

2011-01-2278

Published
09/13/2011Paolo Casoli and Alvin Anthony
Universita di Parma

Manuel Rigosi

Copyright © 2011 SAE International

doi:10.4271/2011-01-2278

ABSTRACT

This paper describes the preliminary results of a study focused on the semi empirical modeling of an excavator's hydraulic pump. From the viewpoint of designing and tuning an efficient control system, the excavator is a very complex nonlinear plant. To design and tune such a complex control system an extremely good nonlinear model of the plant is necessary. The problem of modeling an excavator is considered in this paper; a nonlinear mathematical model of an excavator has been developed using the bond graph methodology realized in the AMESim® simulation software to replicate actual operating conditions. The excavator model is described by two models: a hydraulic model and a kinematic model. At this stage of research the hydraulic model deals solely with the model of the main hydraulic pump, which has been conceived as a semi empirical model. The pump model has been conceived as a grey box model; where the flow compensator and pressure compensator have been modeled as white box models while the actual flow characteristics of the pump as a black box model. The other excavator hydraulic system components comprising of valve block and actuators have been created using generic mathematical models. This approach has been followed to enable the study of the pump's dynamic behavior and interaction with a completely developed kinematic model of the excavator. Dynamic loading of the system has been realized through a 2D kinematic model of the excavator's body elements. The kinematic model comprises of the boom, arm and bucket whilst their respective motions have been defined for a cycle of operation. The dynamic parameters of each element are continuously calculated during an excavation cycle, thereby providing a platform to study the pump's behavior. At this phase of model development the

semi empirical model of the variable displacement pump has been validated on the basis of a set of experimental data collected on a test rig at particular experimental operating conditions. The final objective of this study would be to develop a complete mathematical model of the Excavator Hydraulic Control System and in turn facilitate the study of alternate control strategies towards energy efficient systems. This paper presents the results of this study.

KEY WORDS

Hydraulic Excavator, Semi Empirical Modeling, Variable Displacement Pump

INTRODUCTION

The development of control systems for complex mechanical systems such as large manipulators, mobile cranes and excavators requires the use of powerful software development tools. This is particularly true, where a short commissioning period is desired. Here, the complete control-system must be developed and tested by simulation methods. This requires a comprehensive software package for mechatronic systems, consisting of a modeling and simulation part and a control development part. The simulation of the kinematics and dynamics of multi-body systems is a topic of increasing importance in many industrial branches, due to its potential for reducing costs and that it provides insight into inherent effects governing the systems behavior. At a more detailed level, simulation offers enhanced product assessment, the potential of early stage conceptual testing, and a virtually unlimited spectrum of "what if" analysis [7]. Towards realizing this objective a model comprising of a hydraulic and kinematic systems have been developed. The need to model these systems is

attributed to the inherently nonlinear hydraulic drive, used to achieve precise motion and power control. This choice of drive is imputed to the superior power density of hydraulic systems in comparison to electrical or mechanical drives; regrettably the indigent energy efficiency of these systems is a major drawback. The need for energy efficient systems demands that this potent drive be self adjusting to meet actual load requirements [12]. A method of adjusting these systems to meet load requirements is by controlling the flow of a pump. In this context, variable- displacement axial piston pumps are often used, whereby the displacement of the pump can be varied by tilting a swash plate. This can be achieved fast enough to meet the dynamic demands affected by multiple loads. In this research, a nonlinear pump model has been developed, which takes into account the essential nonlinearities of the system and can be easily adjusted to pumps of different displacement sizes in the same model range. A practical pump model must enable one to examine the dominant characteristics influencing the behavior of the pump. In a load sensing pump this would include the response of the pressure and flow compensators in addition to the sensitivity of swash plate motion which defines the pump's displacement. This model can be conceived in a number of ways either as purely mathematical, empirical or a mix of the two as a semi empirical model. The approach of semi empirical modeling of the pump has been adopted in this paper, thereby providing a basis to rapidly examine different pump sizes to vary the flow gain of a complete excavator with the objective of achieving desired design characteristics. The pump displacement is controlled by the highest pressure feedback generated from the excavator's actuators, in an operating cycle. To subject the pump to these varying forces a detailed model of the kinematics has been realized. Due to the complexity of the whole system, dynamic forces are required for computing the load on the system which is achieved by the kinematic model of the excavator. Previously published research comparisons describe the differences between these static and dynamic forces [7]. The nonlinear effects occurring during the excavation cycle such as the bucket-soil interaction and the nonlinearities of the hydraulic system complicate the control of the pump. These factors have to be taken into account in hydraulic modeling and control. The above details provide a glimpse into the complexity of variable forces that a system would experience during an operating cycle for which the variable pump compensates its displacement. Thus far, having described the objective of this research, the following sections will detail the modeling of the pump, the excavator kinematics and validated results of the pump model.

PHYSICAL MODELING

PUMP MODEL

The pump model described in this paper is that of a load sensing variable displacement axial piston pump. This is a standard line production pump developed by Casappa SpA and belongs to the MVP series. The study of optimal displacement control of variable displacement pumps has been a topic of interest for fluid power researchers' world over and continues to provide scope for development with electro hydraulics and recent advances in robust control strategies. To set the pace of study, this paper describes the current stage of model development and will detail the actual pump being produced, i.e. with classical hydraulic feedback. As depicted in Fig.1, the pump model comprises of three sub-models a flow compensator, pressure compensator and the flow characteristics. The pump model has been conceived as a grey box model, i.e. a model based on both insight into the system and experimental data as can be seen in Fig.2. The flow and pressure compensators have been modeled as white box models and that of the flow characteristics as a black box model. The grey box model of the pump correlates the control piston pressure and the system pressure to provide the equilibrium of forces that defines the swash plate angle. This model approach has been adopted to provide the manufacturer with the flexibility of selecting pumps with discrete maximum displacements to vary the complete system's gain.

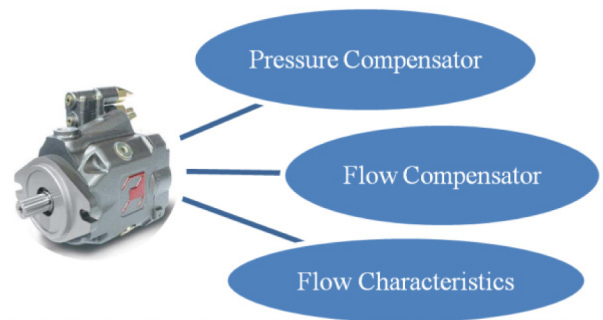


Fig. 1. Model breakup of the MVP series, Load Sensing Variable Displacement Pump

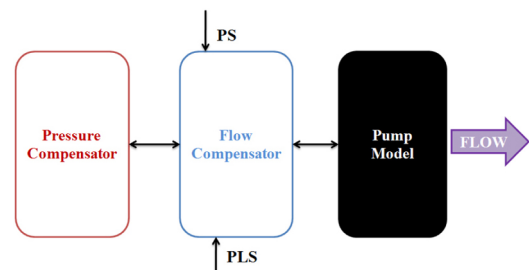


Fig. 2. Grey Box modeling methodology

The mathematical models of the flow compensator, pressure compensator and flow characteristics have been developed using the bond graph methodology realized through the AMESim® simulation software. This methodology uses the transfer of power between elements to describe the dynamics of the system. The basic idea being - the direction of power flow at any moment in a system is invariant. Power may be expressed as a multiplication of two factors - generalized effort and generalized flow. Bond graphs are far more powerful in modeling complex systems which involve the interaction of several energy domains [2].

Flow Compensator Model

The flow compensator (FC) has the most important function of offsetting the pump displacement for a set preload by regulating the swash plate angle. This component has been modeled and verified in great detail [10].

The logic integrated in the FC is to compare the dominant load pressure (PLS) with the pump's output pressure (PS) to modulate the flow through the FC, hence regulating the pump's displacement. The objective of the FC is to maintain a fixed differential pressure across the control orifice accomplished by modulating the pump's flow. The FC's spring comprises of two springs one being a snubber spring. This arrangement has been adopted to provide a snubbing function - thereby resiliently biasing the spool from the first operating position to the second operating position, when the fluid pressure in the LS chamber is increased from a first pressure level to a second pressure level. This feature has an attribute of controlling pressure spikes more carefully due to the precise metering characteristics of the valve, thus reducing the oscillations on the swash plate.

The functioning of the FC as depicted in Fig.3 and Fig.4 is such that the pump pressure enters the FC valve through the chamber A. The pressure entering this chamber acts on the area of spool 1 to create a force. This is realized in the model by means of a transformer element, in the form of spool 1, where the modulus of the transformer is the ratio between the spool - piston and rod area. The force created by the pump pressure on spool 1 is countered by the force created by the springs 5 and the LS pressure which is sensed in chamber D. The sum of these two forces i.e. spring 5 and the LS pressure acting on the area of piston 4 is the force value used to maintain the force balance of the spool. When the pump pressure is greater than the force on piston 4, the spool is displaced to the left creating a flow path between chamber A and chamber B, referred to as the intermediate chamber. The flow through this chamber has the function of varying the pump's swash plate angle, and in this way the pump displacement is regulated. Chamber C is connected to tank and its function is to drain the oil from the intermediate chamber. Spool 2, has been modeled as a transformer element with the modulus being the area ratio between the spool -

piston and rod. Leakage models have been included as depicted in 3 (Fig.4) to describe internal leakage between chambers and to increase the system damping.

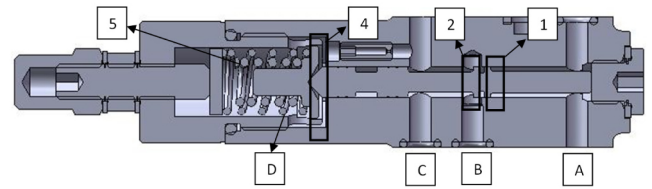


Fig. 3. CAD model of the Flow Compensator

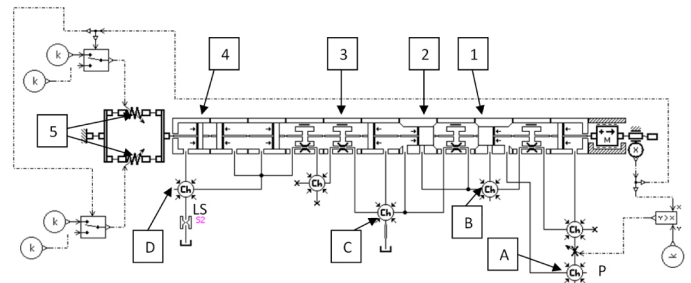


Fig. 4. AMESim® model of the Flow Compensator

The governing equations are described by the interaction between a fluid-dynamic model (FDM) and a mechanical-geometrical model (MGM). The FDM calculates the pressures inside the chambers and the flow rate between adjacent chambers, while the MGM calculates the forces acting on the spool and determines its dynamics and the flow areas.

The FDM is based on a lumped parameter framework. The pressure inside each control volume is assumed uniform and time dependent, and is determined by the pressure-rise rate equation:

$$\frac{dp_i}{dt} = \frac{\beta}{\rho_i} \frac{1}{V_i(x)} \left(\sum \dot{m} - \rho_i \frac{dV_i(x)}{dt} \right) \quad (1)$$

The model assumes a constant value of fluid temperature. The fluid density is evaluated as a function of pressure as described in [8]. The summation term represents the net mass flow rate entering or leaving the volume. This is obtained by considering the contribution of all orifices connected with the considered volume. The mass exchange occurring through the orifices is calculated using the generalized Bernoulli's equation under quasi-steady conditions, Eq. (2):

$$\dot{m} = C_d A(x) \sqrt{\frac{2 |\Delta p|}{\rho}} \quad (2)$$

The user sets an appropriate saturated value for the coefficient of discharge of each connection, on the basis of experimental data or using values reported in literature, such as [8, 9]; thereafter the instantaneous coefficient of discharge value is evaluated as a function of Reynolds number, to account for partially developed or fully turbulent conditions. Annular leakages past spool bodies have been evaluated using Eq. (3) as reported in [8, 9]:

$$\dot{m} = \rho \frac{\pi \cdot R \cdot h^3}{6 \cdot \mu} \cdot \frac{|\Delta p|}{L} \quad (3)$$

The mechanical model calculates the instantaneous position and velocity of the spool using Newton's second law:

$$\sum_i F_i = ma \quad (4)$$

The forces acting on the spool, Fig.4, are: hydrostatic forces; spring force; friction forces; hydrodynamic forces. Static and dynamic friction forces are evaluated by use of the Karnopp friction model and considering the Stribeck effect; static and dynamic friction coefficients are assumed constant; the hydrodynamic forces are proportional to the orifice flow sectional area and pressure drop across the orifice, the model implements the equation:

$$F = 2 \cdot C_d \cdot A \cdot \Delta p \cdot \cos\theta \quad (5)$$

where the jet or flow angle θ is affected by chamber geometry, orifice clearance and sharpness; for spool valves with a sharp edged orifice and no clearance between spool and sleeve, θ can be assumed equal to 69° [3]. The other assumptions are that fluid inertia is neglected; springs are assumed linear.

Pressure Compensator Model

The function of the pressure compensator (PC) is that of a relief valve and its function is to limit the maximum pressure of the system, Fig.5. The relief valve provides an alternate flow path to tank while keeping the system pressure at the relief valve setting. The relief valve realized in the PC is that of the direct operated type, it operates with a spring to preload the valve spool. Since a small flow rate is passed through the spool, the set pressure can be maintained with nearly no effect on the pressure flow characteristics of the

valve. The functioning of the PC is such that the system pressure enters the PC through chamber E (Fig.6) and the pressure acts on the area of spool 6 to create a force, which resists the force created by the spring 8 and spool 9, creating a relief setting pressure. When the system pressure is greater than the relief setting pressure, the spool 6 is displaced and creates a flow path to the swash plate actuating piston and to tank through an orifice S1 (Fig.6), which is housed in the PC valve. The governing equations describing the physical behavior of the PC are the same as those described in the section on the modeling of the flow compensator.

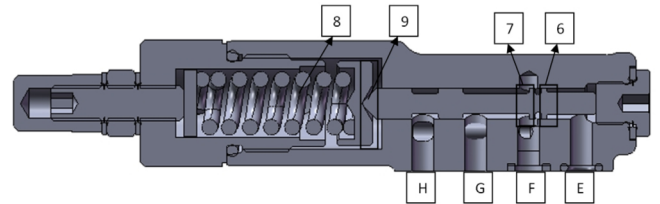


Fig. 5. CAD model of the Pressure Compensator

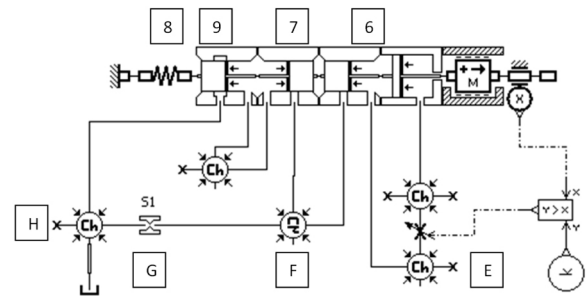


Fig. 6. AMESim® model of the Pressure Compensator

Flow Characteristics Model

A model of the pump's flow characteristics must permit the examination of dominant characteristics influencing the pump's behavior. In a load sensing pump this would include the response of the pressure and flow compensators in addition to the sensitivity of swash plate motion which defines the pump's displacement. Due to intricacies encountered in the control, design and implementation of this type of pump, it is advantageous to have a comprehensive model of the pump. Such a model would include determining the motion of the pump's swash plate based on the instantaneous operating conditions. To achieve this, the model must include the effects of friction acting on internal components, accurate determination of pressure in the pumping pistons and the effects of the swash plate motion on the control actuator. The model must reflect both the supply flow characteristics of the pump as well as the dynamic behavior associated with the internal components in the pump itself.

In practice the accurate prediction of swash plate motion is the exclusive parameter required to represent an axial piston pump, as all pump components interact with the swash plate to determine its motion. The angle of the swash plate determines the stroke of the pumping pistons, the length of which dictates the flow characteristics. The prediction of the swash plate motion is made difficult due to the exciting forces imparted on the swash plate by the pumping pistons as well as the compressibility of the fluid in the control piston. The bond graph model of the pump Fig.7, describes that the net torque acting on the swash plate comprises of the torque contributed by the swash plate inertia, pumping pistons torque, return spring torque, control piston torque and damping effects. These torque values define the swash plate angle to the transformer that modulates the pump's displacement. Regrettably the white box model approach is quite elaborate and does not afford the flexibility required to examine pumps of different sizes as all the constants (piston mass, lengths and diameters, swash plate mass, damping, valve plate geometry etc.) would have to be modified to adopt a different pump.

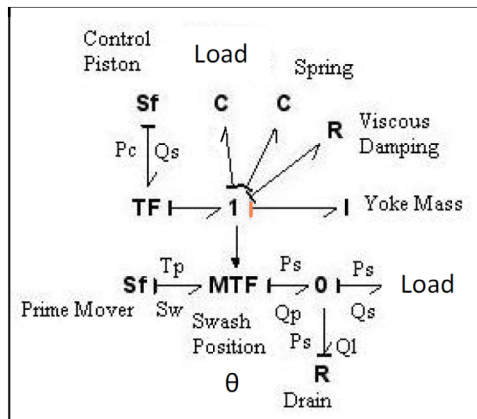


Fig. 7. Bond graph representation of the Pump

The objective of this research has been to adopt a technique for identifying the dominant characteristics of a pump and to facilitate the study of different pump sizes in a feasible manner. This flexibility has been integrated into the model to study the flow gain offered by different pumps to the system. The black box system identification was identified as the best model methodology to integrate this flexibility. This choice of modeling methodology was also attributed to the availability of an instrumented test facility and a large sample of experimental data. The black box model was realized by taking into account that the position of the swash plate could be determined by solely balancing the parameters of the control piston pressure and the system pressure. The control piston pressure is the pressure in the actuator that is used to displace the swash plate. The control piston receives its input from the flow/pressure compensator, depending on the state of the system. The system pressure is the pressure that acts on

the swash plate to determine the forces on it. The forces acting on the swash plate affected by the system pressure comprises of the forces exerted by the pumping pistons exposed to the load and the internal friction forces.

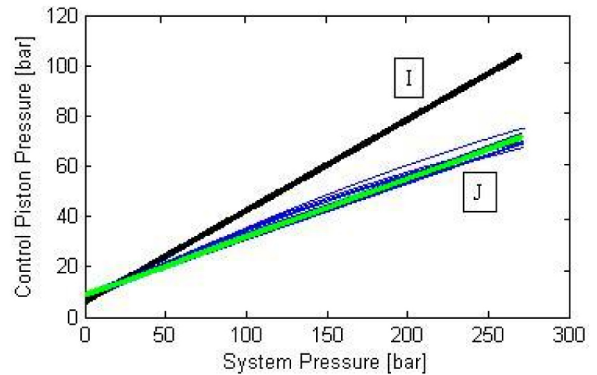


Fig. 8. Correlation between control pressure and system pressure for swash angle position at 1000 r/min

The authors have experimentally obtained a linear relation between the control piston pressure and the system pressure. It was found that the functioning of the pump in different swash angle positions can be defined by two equations. The first equation (6), as depicted in Fig. 8 curve I, describes the control piston pressure (P_C) versus the system pressure (P_S) that would be needed to initially displace the pump from its maximum swash angle position.

$$P_C = 0.362 \cdot P_S + 6.02 \quad (6)$$

The second equation (7) is the pressure balance relation for the intermediate positions. Experiments were carried out by maintaining the swash plate at different positions and varying the load. From these tests it was observed that for the various intermediate swash angle positions, the pressure relationships were found to overlap. Equation (7) was derived by interpolating the family of curves depicted in Fig.8 curve J.

$$P_C = 0.233 \cdot P_S + 8.50 \quad (7)$$

The flow characteristics model has been realized by the use of two pistons - the control piston, 10, and the barrel forces piston, 11 (Figure.10), defined by the system pressure. The relation between these two equations has been realized by a constant value in the simulation model which has been used to switch between the two equations when the swash plate is displaced from its initial position. After the swash plate angle shifts from maximum swash position, the model utilizes a correction factor of 0.644 and a different constant force to modify the pressure relationship described by equation (6) into equation (7). A transformer element in the form of a lever is used to balance the forces from the two pistons. The

linear displacement of the control piston actuator is measured and converted into the swash plate angle. An orifice 13, (Fig. 10) with a fixed area has been used to realize the function of internal leakages of the pump and to simulate the pump's drain characteristics.

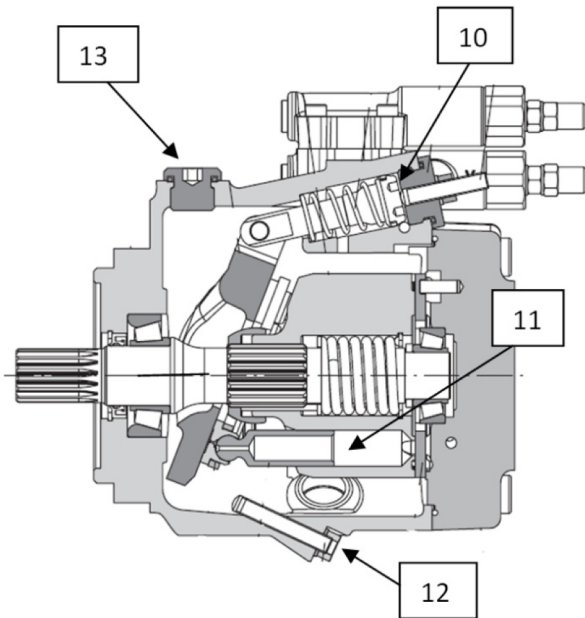


Fig. 9. Cross section view of the swash plate and control piston

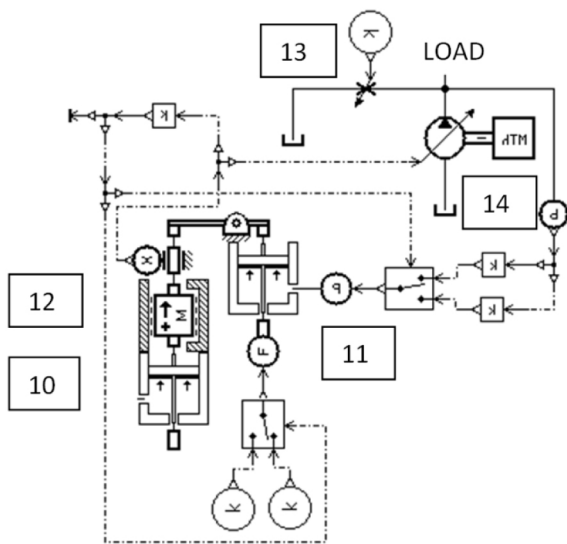


Fig. 10. AMESim® representation of Fig. 9

Although it is known that the leakage flow is a complex term and is best represented experimentally, it was found that the use of a specific flow area provided fairly reliable flow characteristics.

The pump's end stop has been simulated by the use of element 12. The model of the pump's flow characteristics has been created by use of an ideal pump element 14 (Fig.10). The use of the fixed orifice to replicate the drain characteristics provides for fairly reliable flow characteristics. Future work would include maps of the mechanical and volumetric efficiency to replace the drain orifice 13 and to drive the pump's flow characteristics model.

EXCAVATOR DYNAMICS

This section describes the modeling of the excavator kinematics which has been used to create the realistic forces on the hydraulic actuators. Considering the benefits of having the kinematic model integral with the hydraulic model, the linkage parameters were coupled to the hydraulic model using the Planar Mechanics library of AMESim® [4, 6]. This facilitates the understanding of dynamic loads on the hydraulic cylinder. The driving joint torques of the boom, arm and bucket are generated by the forces of the hydraulic ram actuators. The translational and rotational motions of these links are described by the dynamic model of the excavator system. The kinematic model has been incorporated as a lumped parameter model, which accounts for angular position, relative coordinates, distances between links, relative velocity, relative acceleration and the output forces. Joint forces of contact and stiffness, are also considered in the model. The equations of motion can be derived by applying the Euler-Lagrange equations to a Lagrangian energy function. The revolute pairs have been modeled as Lagrange multipliers and are calculated from the Baumgarte stabilization method applied to the constraint equations [11].

To further enhance the force simulation of the model, the visco-elastic properties of the material being handled have been recreated as a force during the excavation process. An impulse force which acts on the bucket during soil penetration has been included as described in [5]. The motion of the excavator implements would be to follow a pre-planned digging trajectory. During digging, three main tangential resistance forces arise: the resistance to soil cutting, the frictional force acting on the bucket surface in contact with the soil and the resistance to movement of the soil ahead of and in the bucket. The magnitude of the digging resistance forces depends on many factors such as the digging angle, volume of the soil, volume of material ripped into the bucket, and the specific resistance to cutting. These factors are generally variable and unavailable. Moreover, due to soil plasticity, spatial variation in soil properties, and potentially severe heterogeneity of material under excavation, it is impossible to exactly define the force needed for certain digging conditions. Accounting for these variable force conditions of the soil by including the parameters from [5] and the study of its effect on the system during the digging

cycle have led to a well developed model of the kinematic system of the excavator.

OVERVIEW OF THE COMPLETE MODEL

Figure 12 depicts the complete model as it is in the present stage of model development. The model is represented in three sections, the first section comprising of the pump model, the second section of the valve blocks and pressure feedback logic and the third section representing the rigid body linkage. As part of the present stage of model development, the pump and kinematics model have been linked together, using valve blocks and pressure compensated flow control valves with ideal characteristics. The pressures across all actuator ports have been compared to provide the maximum load at any instant of time to provide the LS pressure to the FC. The actuators in this model are linear actuators and have been modeled as components which include pressure dynamics in the volumes on either side of the piston, viscous friction, and leakage past the piston. In future work, detailed models of the valve block with compensators and actuators will be included to recreate the complete functioning of the system.

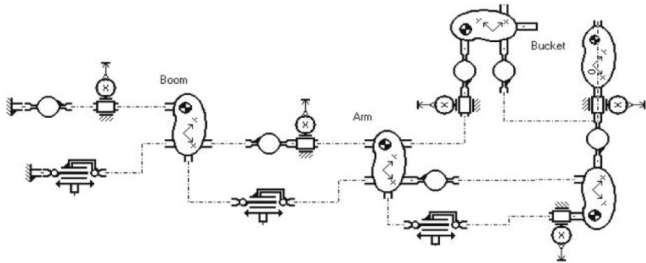


Fig. 11. AMESim® model of the Excavator Kinematics

EXPERIMENTAL TEST SETUP

PUMP EXPERIMENTAL TEST SETUP

The main components of this test stand are the variable displacement axial piston pump P, flow compensator FC, pressure compensator PC, ball valve and the prime mover which is a DC motor. The LS signal is tapped from the output of the ball valve and is measured using sensor P3. The actuator for controlling the swash plate is controlled by the FC/PC valve and the swash plate position is measured using an LVDT. The use of an LVDT to derive an angular value is justified by the fact that in this case, the curvature of the arc representing the swash plate rotation is extremely large and can be represented as a straight line. The system load is generated by a proportional relief valve, rated for 315 bar maximum pressure with a capacity to control the pressure for an inputted constant or mathematical function. The schematic diagram of the hydraulic circuit of the test facility is as

depicted in Fig. 13 and the instrumentation used on the system is summarized in Table.1. Figure 14 is a photograph of the pump mounted on the test facility. The test rig is also equipped with an off line circuit (not represented in Fig.13) for oil temperature control, constituted by a system of heat exchangers, electronically regulated over a specified working temperature.

COMPARISON BETWEEN EXPERIMENTAL AND SIMULATION RESULTS

LOAD SENSING PUMP

Comparison of Results - Preliminary Tests

The complete model of the pump was verified by experimental results. The load pressure values (Fig.15), which comprised of a cyclic pressure loading was obtained from experimental test and were used to drive the simulation pump model's load characteristics. The other controlled parameter was that of the ball valve used to control the orifice opening (Fig.16). A random input was used to study the simulation models ability to reproduce intermediate swash plate positions. In effect the model was subjected to two varying inputs to verify the reproducibility of the pump parameters. The parameters that were verified to develop confidence in the reproducibility of the pump dynamics were that of the swash plate displacement and the pressure characteristics of the control piston. This was verified in experimental results, by use of a LVDT which was mounted directly on the swash plate. The rotation of the swash plate was approximated as linear, as the angle of rotation is small. Figure 17 represents the swash plate position of the pump; Fig.18 describes the output flow of the pump. Figure 19 represents the control piston pressure. The actual control pressure plots are noisy, this is attributed to the pumping frequency and have been fitted in Fig.19 to represent the correlation. Fig. 20, describes the spool displacement of the FC valve. The FC valve provides a flow path when the displacement value exceeds 3.90mm. Figures 17,18,19 present the verification of simulation results against the actual test data. It is evident that there is a good relation between the simulation and experimental results.

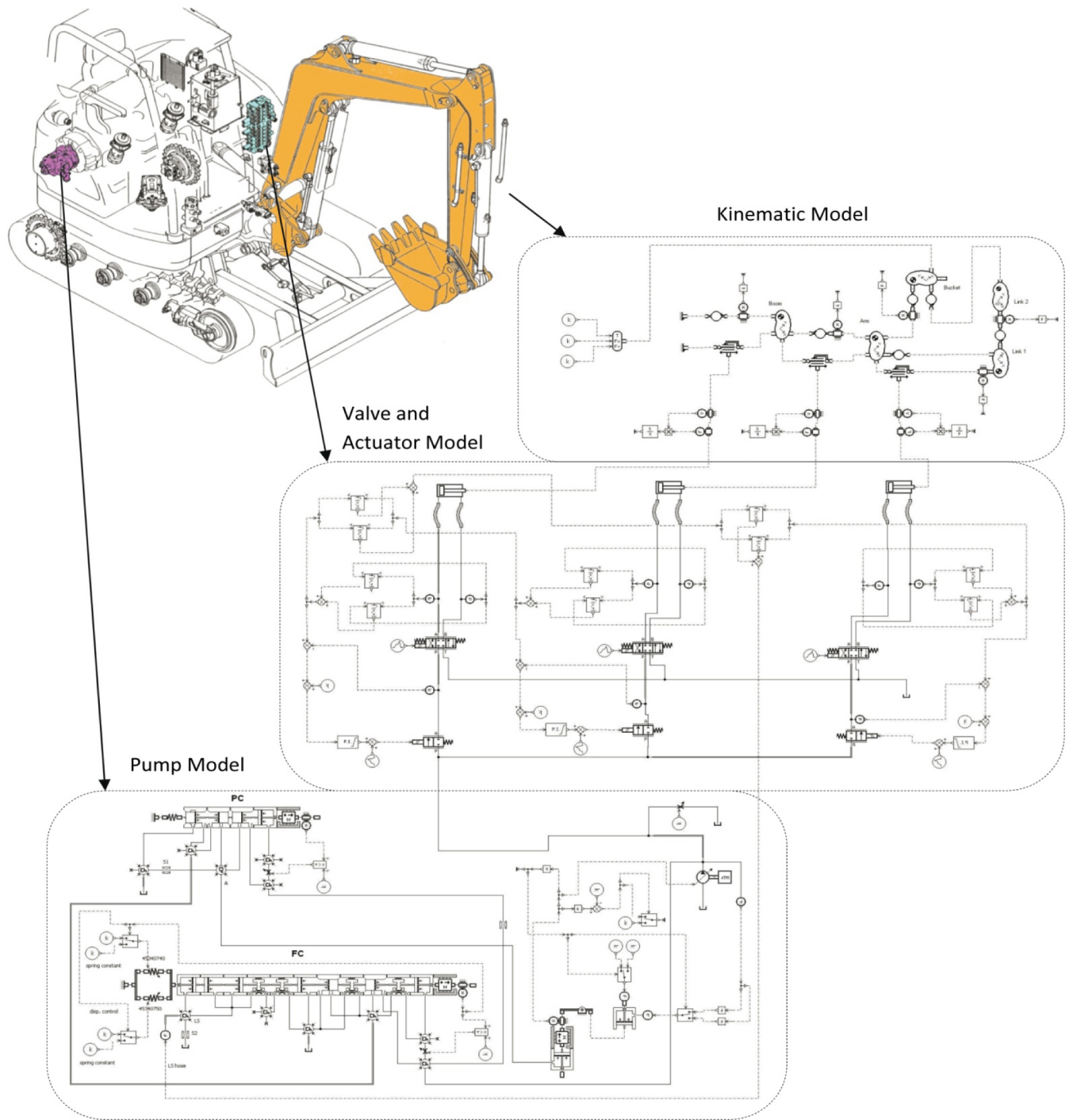


Fig. 12. Overview of the Complete Model

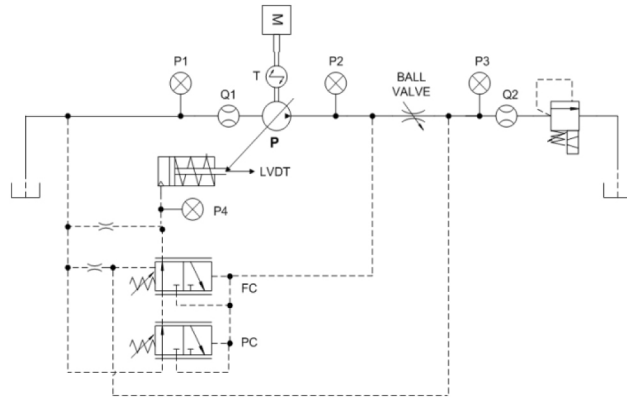


Fig. 13. Test setup for Load Sensing Variable Displacement pump testing

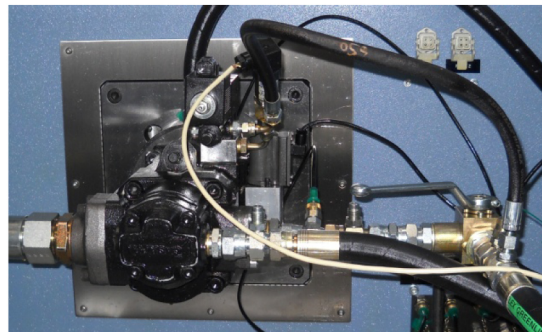


Fig. 14. Photograph of the pump with compensators mounted on the test bench

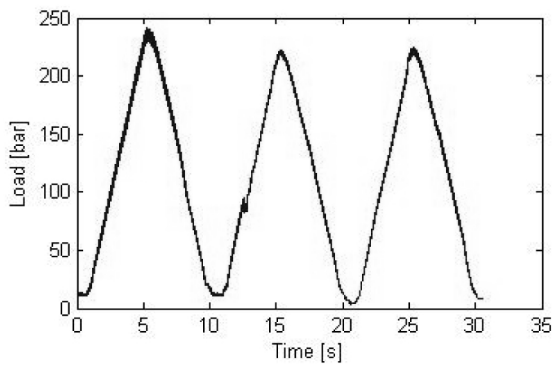


Fig. 15. Load pressure cycle

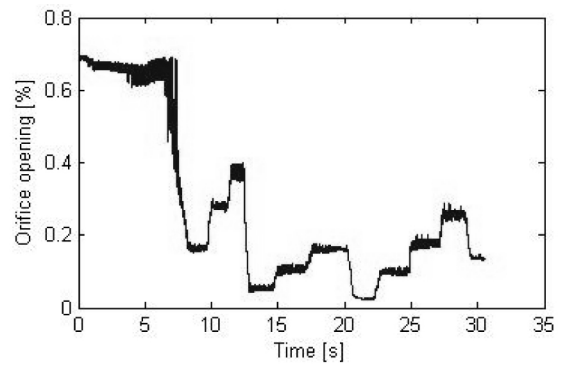


Fig. 16. Orifice opening

Table 1. Features of sensors and main elements of the apparatus used in the present research

Sensor	Type	Main features
M	Prime mover	ABB [®] , 4-quadrant electric motor, 75 Kw
P	Pump	CASAPPA [®] MVP60, 84 cm ³ /r
P1	Strain gage	WIKA [®] , Scale: 0..40 bar, 0.25% FS accuracy
P2 – P3 – P4	Strain gage	WIKA [®] , Scale 0..400 bar, 0.25% FS accuracy
Q1, Q2	Flow meter	VSE [®] VS1, Scale 0.05..80 l/min, 0.3% measured value accuracy
T	Torque/speed meter	HBM [®] T, Scale: 0..500 Nm, 12000 r/min Limit Velocity, 0.05 Accuracy Class
θ	Incremental encoder	HEIDENHAIN [®] ERN120, 3600 imp./r, 4000 r/min Limit velocity, 1/20 period accuracy

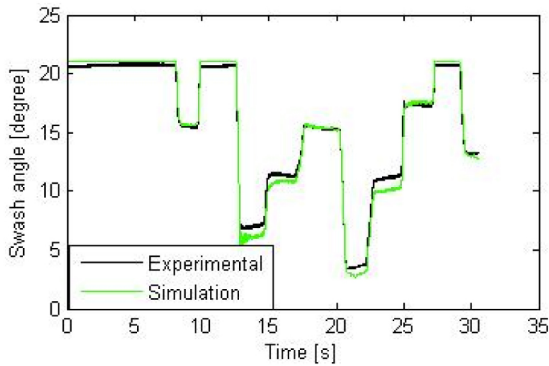


Fig. 17. Comparison between experimental and simulation swash angle

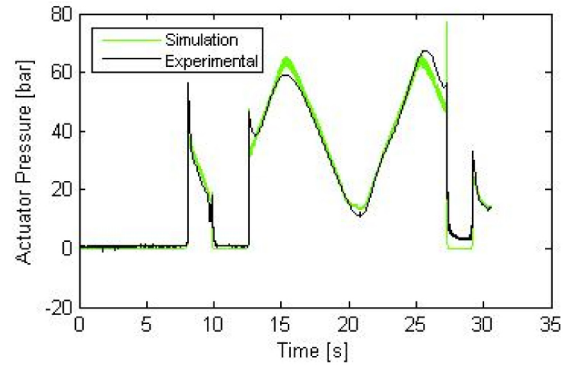


Fig. 19. Comparison between experimental and simulation actuator pressure

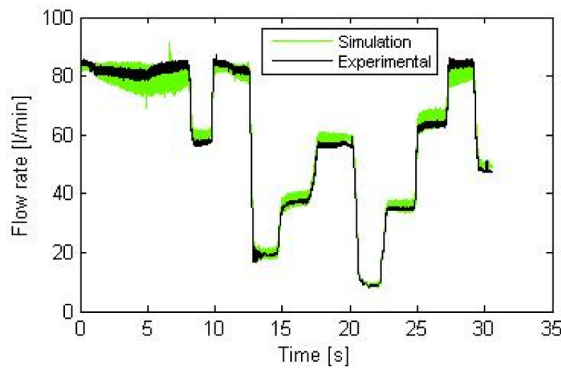


Fig. 18. Comparison between experimental and simulation flow rate

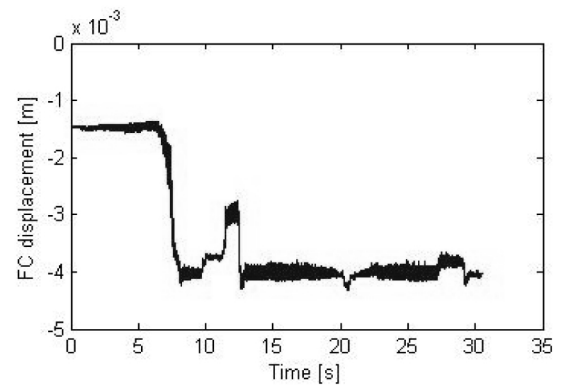


Fig. 20. Flow compensator simulated displacement

Table 2. Duty cycle - Control Signals to Valve Block for Boom, Arm, Bucket Motion

Implement Name	Time [s]	Valve Opening [%]	Actuator Action
Boom	0 - 2	0 - 30 (ramp)	Retraction
	2 - 7	0	-
	7 - 10	0 - 30 (ramp)	Extension
	10 - 13	0	-
Arm	0 - 2.5	0	-
	2.5 - 7.5	100 - 50 (ramp)	Extension
	7.5 - 10	0 - 50 (ramp)	Retraction
	10 - 13	0	-
Bucket	0 - 2.5	0	-
	2.5 - 7.5	100	Extension
	7.5 - 10	0	-
	10 - 13	0 - 50	Retraction

EXCAVATOR MODEL

Excavator Model Executing a Digging Cycle with Boom, Arm and Bucket

On analysis of results presented in the previous section, it is evident that the pump model is capable of reproducing actual conditions. Thus the model was extended to include the valve blocks and the kinematics as depicted in Fig.12 and described in section 2.3. The complete system was subjected to a duty cycle as described in Table.2. The values from Table.2 were used to control the valve opening for respective implements. The pump's maximum displacement used for this simulation was 84 cm³/rev and the engine speed was set at 1000 rev/min. Figure 21 describes the initial condition of the excavator in the simulation model. Figure 22 describes the forces on the implements and the effects of these forces can be seen in Figs. 23, 24 and 25 in pressure terms on the boom, arm and bucket actuators. Figure 26 describes the pressures across the FC, as it can be seen the LS pressure is the instantaneous maximum pressure of the system derived from the actuators and the pump pressure is the instantaneous system pressure. Figure 27 describes the differential pressure across the FC, that is equal to the pump margin set to about 17 bar. Figures 28 and 29 describe the spool displacements of the PC and FC respectively: the FC provides a flow path through the spool when the displacement is greater than 3.90 mm and the PC when the displacement is greater than 2.10mm. Figure 30 describes the pump swash angle controlled by the flow across the FC and PC spools.

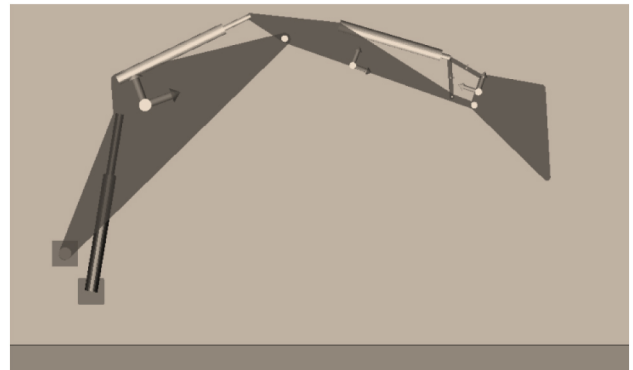


Fig. 21. Initial position of the Excavator

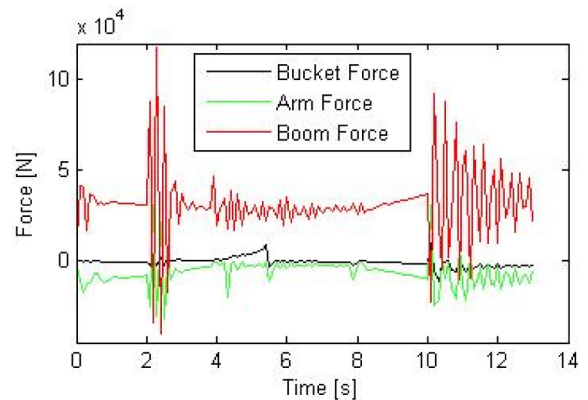


Fig. 22. Actuator Forces

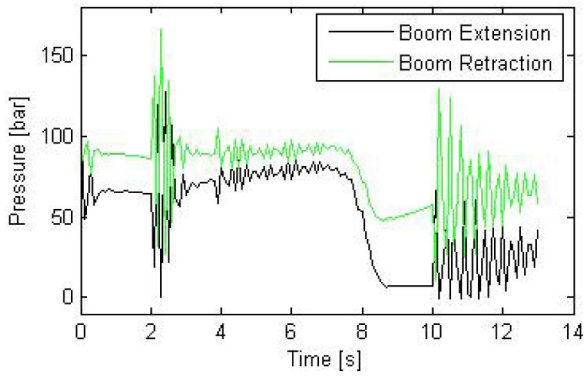


Fig. 23. Pressure in Boom Actuator

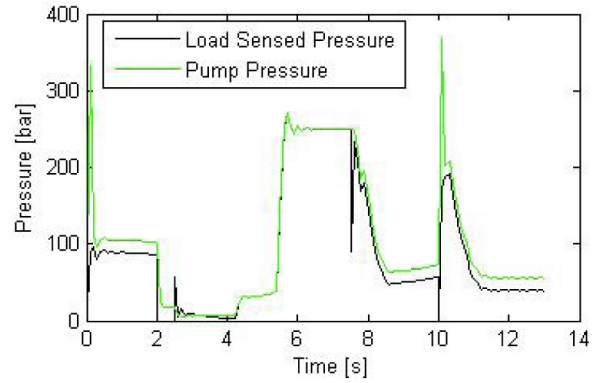


Fig. 26. Pressure Across the FC

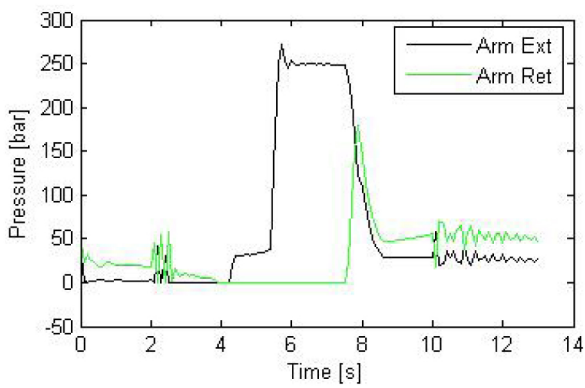


Fig. 24. Pressure in Arm Actuator

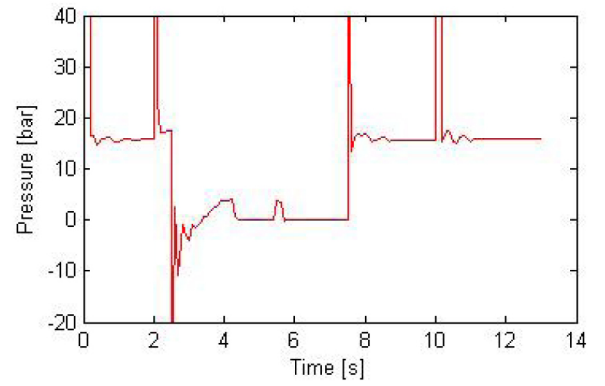


Fig. 27. Differential pressure across the FC

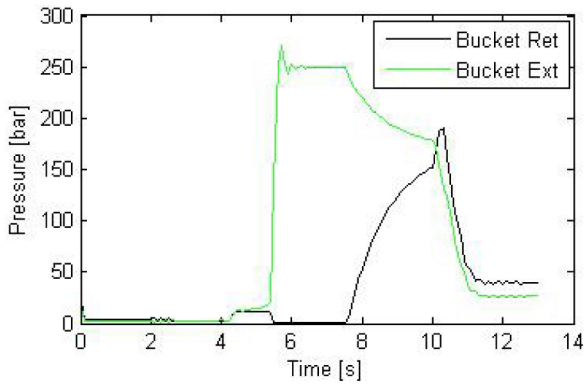


Fig. 25. Pressure in Bucket Actuator

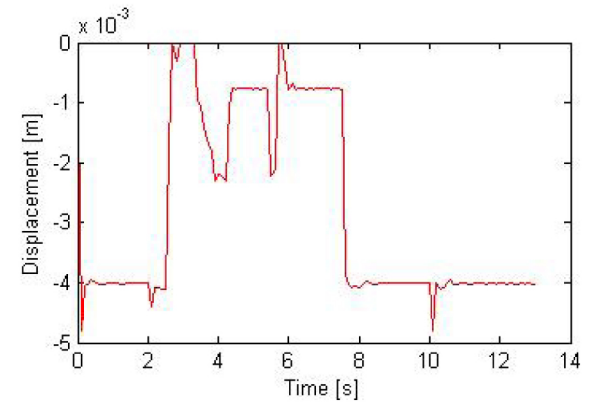


Fig. 28. Displacement of the FC

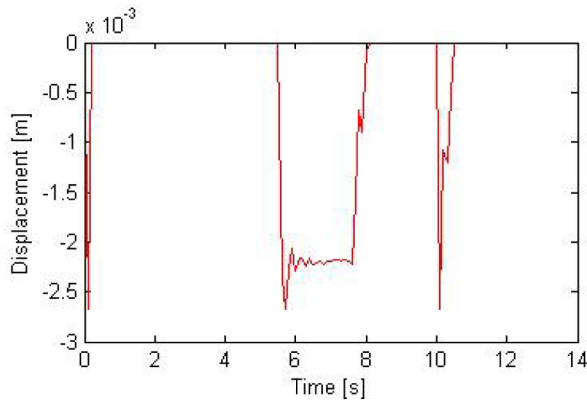


Fig. 29. Displacement of the PC

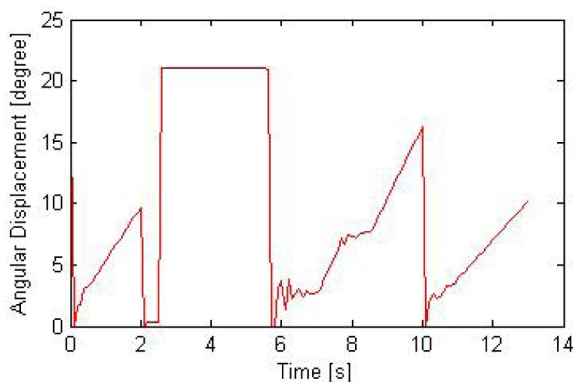


Fig. 30. Swash Angle

SUMMARY/CONCLUSIONS

The paper has presented the analysis of an excavator control system. A nonlinear mathematical model of an excavator has been developed using the AMESim® modeling environment to replicate actual operating conditions. The model is described by two models: hydraulic grey box model and a 2D kinematic model to simulate the excavator's body elements. This approach has enabled the study of the dynamic behavior and interaction of the pump with a completely developed kinematic model of the excavator. The detailed hydraulic model described is that of the main hydraulic pump, which has been conceived as a grey box model; where the flow and pressure compensators have been modeled as white box models and the actual flow characteristics of the pump as a black box model. The black box model to obtain the swash plate positions has been developed using a relation between the control piston pressure and the net torque acting on the swash plate through the system pressure. A linear relation between these pressure characteristics were derived from experimental results and was used to simulate the functioning of the pump. This methodology has the advantage of being easily applicable to pumps of different types and sizes. The model of the variable displacement pump has been validated on the basis of a set of experimental data collected at

particular operating conditions. It has permitted the necessary verification of the pump's behavior and provides confidence in the expected interaction between the hydraulic and kinematic model. Therefore the authors are confident to bring the study forward and assess a set of strategies aimed to improving the control of the system and the overall system efficiency.

REFERENCES

1. Anthony, Alvin Casoli, Paolo Vacca, Andrea. (2010). *Analysis of a tractor rear hitch control system*. Proc. Of 6th FPNI-PhD Symposium West Lafayette, 15-19 June 2010, pp. 589-602. FPNI Fluid Power Net Publications, 2010
2. Mukherjee, Amalendu Karmakar, Ranjit Samatry, A.K. (2006) *Bond Graph in Modeling Simulation and Fault Identification*, I.K International Publishing House
3. Blakburn, J. F., Reethof, G. & Shearer, J. L. (1966) *Fluid Power Control*. USA: MIT Press, 1966. ISBN 0262520044.
4. Casoli, P., Vacca, A., Anthony, A., Berta, G.L. (2010). *Numerical and Experimental Analysis of the Hydraulic Circuit for the Rear Hitch Control in Agricultural Tractors*. 7th International Fluid Power Conference, (pp. 51-63, vol. 1) Aachen, 22-24/03 2010, ISBN 978-3-940565-90-7
5. Grzesikiewicz, W. (1998). *Dynamics of a ground digging tool*. XI scientific Conference Problems of Work Machines, konferencja Naukowa Problem Maszyn Roboczych) Polska: Zakopane, 1998
6. LMS Imagine - AMESim® Reference manual 2009
7. Hiller, Manfred. (1996). *Modeling, simulation and control design for large and heavy manipulators*, Journal of Robotics and Autonomous Systems 19 (1996) 167-177
8. McCloy, D., Martin, H. M. (1973). *The control of Fluid Power*, Longman, London, 1973
9. Merrit, H.E. (1967) *Hydraulic Control Systems*, Wiley, New York.
10. Casoli, Paolo Anthony, Alvin *Modeling of an Excavator - Pump Nonlinear Model and Structural Linkage/Mechanical Model*, Proc. Of 12th Scandinavian International Conference on Fluid Power, May 18-20, 2011, Tampere, Finland
11. Lin, Shih-Tin. (2002) *Stabilization of Baumgarte's Method Using the Runge-Kutta Approach*, ASME Journal of Mechanical Design, December 2002
12. Wu, D., Burton, R., Schoenau, G., Bitner, D. (2007), *Analysis of a Pressure -Compensated Flow Control Valve*, ASME Journal of Dynamic Systems, Measurement and Control, March 2007

CONTACT INFORMATION

Paolo Casoli
Paolo.casoli@unipr.it

Alvin Anthony
Alvinanthony7@gmail.com

ACKNOWLEDGMENTS

The authors would like to acknowledge the active support of this research by Casappa SpA., Parma, ITALY.

DEFINITIONS/ABBREVIATIONS

A	flow area
a	acceleration
C_d	discharge coefficient
F	force
h	gap height
i	volume index
m	mass
\dot{m}	mass flow rate
P	Pressure
P_c	Control Piston Pressure
P_s	System Pressure

Q_l	Leakage Flow
Q_s	Load Flow
R	Radius
L	length of the leakage
V	Volume
t	Time

Greek Letters

β	bulk modulus
μ	dynamic viscosity
ρ	density

Acronyms

FC	Flow compensator
PC	Pressure compensator
PS	System Pressure
PLS	Load Sensed Pressure